Article

Iminosugar Glycosidase Inhibitors: Structural and Thermodynamic Dissection of the Binding of Isofagomine and 1-Deoxynojirimycin to β-Glucosidases

David L. Zechel, Alisdair B. Boraston, Tracey Gloster, Catherine M. Boraston, James M. Macdonald, D. Matthew G. Tilbrook, Robert V. Stick, and Gideon J. Davies

J. Am. Chem. Soc., **2003**, 125 (47), 14313-14323• DOI: 10.1021/ja036833h • Publication Date (Web): 04 November 2003

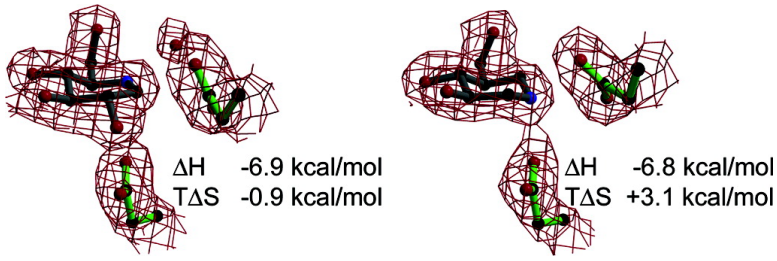

More About This Article

Additional resources and features associated with this article are available within the HTML version:

- Supporting Information
- Links to the 14 articles that cite this article, as of the time of this article download
- Access to high resolution figures
- Links to articles and content related to this article
- Copyright permission to reproduce figures and/or text from this article

View the Full Text HTML

J|A|C|S
ARTICLES
Published on Web 11/04/2003

Iminosugar Glycosidase Inhibitors: Structural and Thermodynamic Dissection of the Binding of Isofagomine and 1-Deoxynojirimycin to β-Glucosidases

David L. Zechel,[†,§] Alisdair B. Boraston,[†,||] Tracey Gloster,[†] Catherine M. Boraston,[†] James M. Macdonald,[‡] D. Matthew G. Tilbrook,[‡] Robert V. Stick,[‡] and Gideon J. Davies*[,†]

Contribution from the Structural Biology Laboratory, Department of Chemistry, University of York, Heslington, York, YO10 5YW, United Kingdom, and School of Biomedical and Chemical Sciences, The University of Western Australia, 35 Stirling Hwy, Crawley WA 6009, Australia

Received June 23, 2003; E-mail: davies@ysbl.york.ac.uk

Abstract: The design and synthesis of transition-state mimics reflects the growing need both to understand enzymatic catalysis and to influence strategies for therapeutic intervention. Iminosugars are among the most potent inhibitors of glycosidases. Here, the binding of 1-deoxynojirimycin and (+)-isofagomine to the "family GH-1" β-glucosidase of *Thermotoga maritima* is investigated by kinetic analysis, isothermal titration calorimetry, and X-ray crystallography. The binding of both of these iminosugar inhibitors is driven by a large and favorable enthalpy. The greater inhibitory power of isofagomine, relative to 1-deoxynojirimycin, however, resides in its significantly more favorable entropy; indeed the differing thermodynamic signatures of these inhibitors are further highlighted by the markedly different heat capacity values for binding. The pH dependence of catalysis and of inhibition suggests that the inhibitory species are protonated inhibitors bound to enzymes whose acid/base and nucleophile are ionized, while calorimetry indicates that one proton is released from the enzyme upon binding at the pH optimum of catalysis (pH 5.8). Given that these results contradict earlier proposals that the binding of racemic isofagomine to sweet almond β-glucosidase was entropically driven (Bülow, A. et al. *J. Am. Chem. Soc.* **2000**, *122*, 8567−8568), we reinvestigated the binding of 1-deoxynojirimycin and isofagomine to the sweet almond enzyme. Calorimetry confirms that the binding of isofagomine to sweet almond β-glucosidases is, as observed for the *T. maritima* enzyme, driven by a large favorable enthalpy. The crystallographic structures of the native *T. maritima* β-glucosidase, and its complexes with isofagomine and 1-deoxynojirimycin, all at ∼2.1 Å resolution, reveal that additional ordering of bound solvent may present an entropic penalty to 1-deoxynojirimycin binding that does not penalize isofagomine.

Transition-state analogue design[1] is a rapidly expanding genre in the glycosidase field.[2,8,26] It is not merely inspired by the design of potential therapeutics, but also by a need to understand transition-state stabilization by this remarkable class of enzyme, which is estimated to accelerate glycosidic bond hydrolysis by a factor of 10^{17}.[3−5] The transition states for enzymatic glycosidase hydrolysis feature considerable oxocarbenium-ion character in which the anomeric carbon acquires sp^2 hybridization and partial positive charge develops at the anomeric carbon and the endocyclic oxygen (Scheme 1).[6] The exact charge distribution and the conformation of the transition state will vary from enzyme to enzyme, in some cases considerably.[7,33] Iminosugars such as 1-deoxynojirimycin (**1**) and isofagomine (**2**) are of particular interest in inhibitor design (Scheme 1). These are often powerful inhibitors of glycosidase action, and it has been proposed that their conjugate acids mirror positive charge development at the endocyclic oxygen or the anomeric carbon of the glycosidase transition state, respectively.[8] While superficially this is a persuasive and intuitive proposal, there is no correlation between K_i and k_{cat}/K_M for **1** and family 1 β-glucosidases.[9,10] Likewise, recent van't Hoff analyses of the

[†] University of York.
[‡] The University of Western Australia.
[§] Current address: Biochemisches Institut, Universität Zürich, Winterthurerstrasse 190, CH-8057, Zürich, Switzerland.
[||] Current address: Department of Biochemistry & Microbiology, University of Victoria, P.O. Box 3055 STN CSC, Victoria, B.C., V8W 3P6, Canada.

(1) Bartlett, P. A.; Mader, M. M. *Chem. Rev.* **1997**, *97*, 1281−1301.
(2) (a) Lillelund, V. H.; Jensen, H. H.; Liang, X.; Bols, M. *Chem. Rev.* **2002**, *102*, 515−553. (b) Heightman, T. D.; Vasella, A. T. *Angew. Chem., Int. Ed.* **1999**, *38*, 750−770. (c) Ganem, B. *Acc. Chem. Res.* **1996**, *29*, 340−347.
(3) Wolfenden, R.; Lu, X.; Young, G. *J. Am. Chem. Soc.* **1998**, *120*, 6814−6815.
(4) Wolfenden, R.; Snider, M.; Ridgway, C.; Miller, B. *J. Am. Chem. Soc.* **1999**, *121*, 7419−7420.
(5) Wolfenden, R.; Snider, M. J. *Acc. Chem. Res.* **2001**, *34*, 938−945.
(6) Zechel, D. L.; Withers, S. G. *Acc. Chem. Res.* **2000**, *33*, 11−18.
(7) (a) Varrot, A.; Davies, G. J. *Acta Crystallogr., Sect. D* **2003**, *59*, 447−452. (b) Ducros, V. M.-A.; Zechel, D. L.; Murshudov, G. N.; Gilbert, H. J.; Szabó, L.; Stoll, D.; Withers, S. G.; Davies, G. J. *Angew. Chem., Int. Ed.* **2002**, *41*, 2824. (c) Sidhu, G.; Withers, S. G.; Nguyen, N. T.; McIntosh, L. P.; Ziser, L.; Brayer, G. D. *Biochemistry* **1999**, *38*, 5346−5354.
(8) Bols, M. *Acc. Chem. Res.* **1998**, *31*, 1−8.

Scheme 1. Transition State for the Glycosylation Step of a Retaining Glycosidase and the Transition-State Analogues 1-Deoxynojirimycin (**1**) and Isofagomine (**2**)

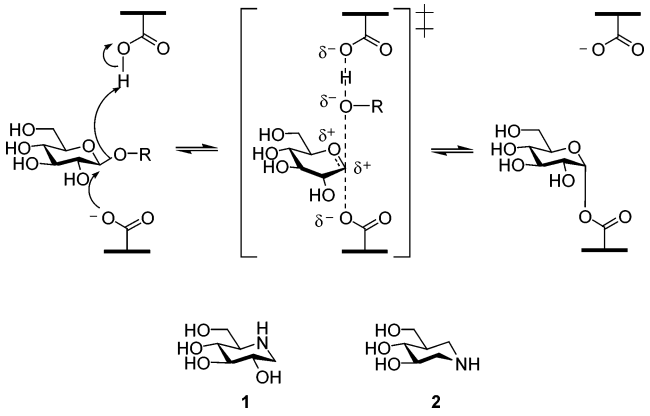

temperature dependence of binding of **1** and racemic **2** to sweet almond β-glucosidase (also a family 1 enzyme[11]) suggest that while the affinity of **1** was enthalpically driven ($\Delta H = -6.14$ kcal mol^{-1}, $T\Delta S = +0.092$ kcal/mol), the affinity of **2** was favored only by entropic forces offset by a greatly unfavorable enthalpy ($\Delta H = +14$ kcal/mol, $T\Delta S = +23.1$ kcal/mol).[12] Given that **1** and **2** most likely make many similar interactions with the enzyme, the large unfavorable enthalpy proposed for **2** is certainly unexpected. Moreover, the thermodynamic parameters for **2** are at odds with a criterion for transition-state analogues proposed by Wolfenden,[4,5] which suggests that the affinity of an enzyme for a transition-state mimic should necessarily be driven by a large and favorable change in enthalpy, as is the case for the corresponding affinity for the reaction transition state.

These observations question the degree, if any, of transition-state mimicry displayed by simple iminosugars and have led us to reexamine the binding of **1** and **2** to family 1 β-glucosidases on the basis of thermodynamics, pH dependence, and three-dimensional structures. Given the known heterogeneity of sweet almond β-glucosidase preparations,[11,13] a β-glucosidase from *Thermotoga maritima* (hereafter *Tm*GH1) was cloned and overexpressed in *Escherichia coli*. Isothermal titration calorimetry (ITC), a technique that directly measures enthalpies of association, reveals that, in contrast to previous suggestions,[12] the binding of **1** and optically pure (+)-**2** is driven by large favorable enthalpies both with the *Tm*GH1 and with the sweet almond enzyme. While **1** and **2** both display similar and favorable enthalpies of binding, the large difference in affinity of the two compounds is indeed governed by the more favorable entropy of **2**. The three-dimensional structure of *Tm*GH1, determined by X-ray crystallography at 2.1 Å resolution in native form, and in complexes with **1**, **2**, as well as a 2-deoxy-2-fluoro-D-glucosyl intermediate, illuminates the different binding properties of these inhibitors, particularly the role of solvation, the 2-hydroxyl, and the acid/base catalyst. The pH profiles for both inhibition and catalysis, and calorimetric

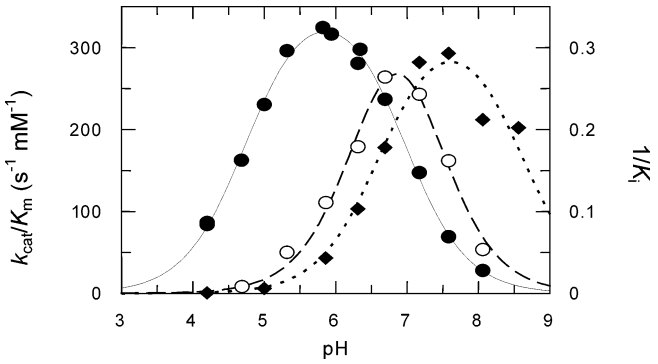

Figure 1. pH dependence of k_{cat}/K_m (2,4-DNP-β-glucoside, ●) and $1/K_i$ (**1**, ○, μM^{-1}; **2**, ◆, nM^{-1}) for *Tm*GH1.

measurements of proton release, suggest that the inhibitory species for **2** is that with protonated inhibitor and a largely inactive enzyme species whose acid/base and nucleophile are both deprotonated. We suggest that the superior inhibition of **2** relative to **1** is not the result of superior transition-state mimicry but is due to an entropic advantage and a more favorable electrostatic interaction with the acid/base catalyst.

Results and Discussion

Cloning, Overexpression, and Kinetic Characterization of *Tm*GH1. Previous intriguing results with almond β-glucosidase led us to investigate the binding of **1** and **2**[14] to β-glucosidases by calorimetry and X-ray crystallography. The sweet almond enzyme, a family 1 glycosidase, is, however, both heterogeneous and predominantly (>50%) inactive.[15] The *T. maritima* family GH-1 β-glucosidase (*Tm*GH1) gene was therefore obtained by PCR on *T. maritima* genomic DNA and overexpressed in *E. coli*. Preliminary studies revealed that, as expected, *Tm*GH1 is highly thermostable, retaining full activity after 4 h and 75% activity after 24 h at 80 °C. Active-site titration of *Tm*GH1 using 2,4-dinitrophenyl 2-deoxy-2-fluoro-β-D-glucopyranoside revealed stoichiometric labeling of enzyme. ESI mass-spectrometry (not shown) gave masses of 51 750 and 51 584 Da for labeled and unlabeled native *Tm*GH1, respectively, with 100% conversion of either enzyme form to the covalent intermediate. The mass difference of 166 Da is exactly that expected for a single 2-fluoro-glucosyl moiety on the labeled enzyme, and 3-D structure analysis, below, confirmed labeling of the catalytic nucleophile Glu351. *Tm*GH1 activity, measured spectrophotometrically using 2,4-dinitrophenyl-β-D-glucopyranoside as substrate (100 mM sodium phosphate, pH 7.0, 25 °C), gave kinetic parameters of $k_{cat} = 42 \pm 1$ s^{-1} and $K_M = 0.41 \pm 0.03$ mM.

pH Dependence of Activity and Inhibition of *Tm*GH1. Values of k_{cat}/K_M at each pH for the reaction of *Tm*GH1 with 2,4-DNP-β-glucoside were calculated from first-order rate

(9) Withers, S. G.; Namchuk, M.; Mosi, R. In *Iminosugars as glycosidase inhibitors: nojirimycin and beyond*; Stutz, A. E., Ed.; Wiley-VCH: Weinheim, 1999; pp 188−206.
(10) Dale, M. P.; Ensley, H. E.; Kern, K.; Sastry, K. A.; Byers, L. D. *Biochemistry* **1985**, *24*, 3530−3539.
(11) He, S.; Withers, S. G. *J. Biol. Chem.* **1997**, *272*, 24864−24867.
(12) Bülow, A.; Plesner, I. W.; Bols, M. *J. Am. Chem. Soc.* **2000**, *122*, 8567−8568.
(13) Legler, G. *Hoppe-Seyler's Z. Physiol. Chem.* **1970**, *351*, 25−31.

(14) **1** was purchased from Toronto Research Chemicals. Optically pure **2** was used in this work, synthesized from L-xylose (Best, W. M.; Macdonald, J. M.; Skelton, B. W.; Stick, R. V.; Tilbrook, D. M. G.; White, A. H. *Can. J. Chem.* **2002**, *80*, 857−865).

(15) Chromatographically pure almond β-glucosidase as purchased from Sigma is a mixture of isozymes belonging to glycosidase family 1 (see ref 11). The material is subjected to lyophilization in the absence of salts, which may partly denature the enzyme. Stoichiometries of 1.7 and 1.0 were shown by affinity labeling of purified isozymes A and B, respectively, which had not been subjected to lyophilization.[13] In a recent attempt to titrate the active sites of SIGMA almond β-glucosidase using ^{13}C NMR, a stoichiometry of 0.95 was observed (Hansen, S. U.; Plesner, I. W.; Bols, M. *ChemBioChem* **2000**, *1*, 177−180). However, the mass of the dimeric enzyme (MW = 135 000 Da) was erroneously used in this calculation, thus in reality only 0.475 equiv of inhibitor bound per monomer (MW = 67 000 Da).

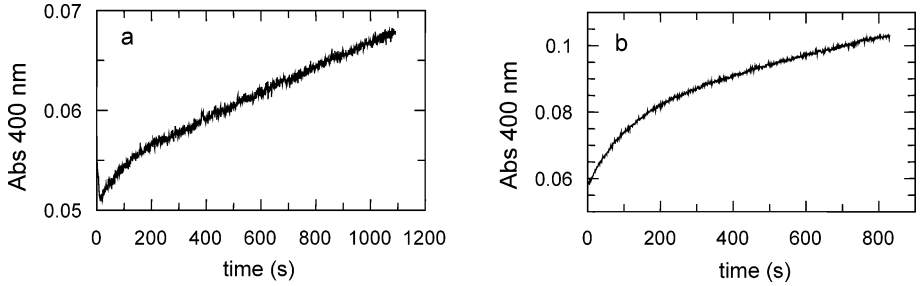

Figure 2. Slow-onset inhibition of *Tm*GH1 with **2** at different pH values (25 °C, [2,4-DNP β-glucoside] = 21 μM). (a) pH 4.2 (K_i = 1.9 μM, [I] = 13.3 μM); (b) pH 5.9 (K_i = 23 nM, [I] = 73 nM).

curves generated at low substrate concentrations ([S] $\ll K_M$). *Tm*GH1 has maximal activity at pH 5.85, with acid and basic limbs displaying pK_a's of 4.75 (±0.03) and 6.96 (±0.03), respectively (Figure 1), very similar to the values reported for the sweet almond enzyme.[16] As with other related systems,[17−20] this pH profile most likely represents titration of the nucleophile and acid/base, respectively.

While linear steady-state rates were observed for *Tm*GH1 in the presence of **1**, slow-onset inhibition was observed for **2** at all pH values, even when the K_i had increased to low micromolar values (Figure 2). This suggests that the slow-onset inhibition of **2** is not merely a phenomenon of tight binding or the use of very low concentrations of inhibitor.[21] Instead, this is more consistent with a unique mechanism of binding, perhaps mediated through a slow conformational change in the enzyme or an unusual change of ionization state of catalytic residues. Slow-onset inhibition with **2** is also observed with the sweet almond enzyme which was attributed to slow bimolecular association with the enzyme.[22] Others, based on fluorescence studies, suggest that slow-onset inhibition of almond β-glucosidase may arise from a conformational change in the enzyme that leads to a high affinity complex.[23,26] Interestingly, unlike **1**, the parent compound nojirimycin exhibits slow-onset inhibition with the almond enzyme, as well as some 50-fold higher affinity.[26]

The pH dependencies of inhibition of *Tm*GH1 with **1** and **2** also follow bell-shaped profiles but with pH optima of inhibition that are alkaline shifted relative to the pH optimum of catalysis for the enzyme (Figure 1). The pH profile for **1** has acid and basic limbs of pK_a's 6.4 (±0.1) and 7.3 (±0.1), respectively, and a maximal K_i value of 3.8 μM (pH 6.85). The profile for **2** is more alkaline shifted, with pK_a's of 6.6 (±0.1) and 8.6 (±0.2) and a maximal K_i value of 3.4 nM (pH 7.6). The K_i values for both inhibitors increase at the pH optimum of *Tm*GH1 (9 μM for **1**, 23 nM for **2**, pH 5.85). As with the previous analyses of the binding of a cellobio-derived **2** to the cellulase Cel5A[20] and the binding of iminosugars to an arabinofuranosidase,[24] the pH dependence of $1/K_i$ for **2** is most simply interpreted in terms of the protonated inhibitor binding to an enzyme species both of whose catalytic carboxylates are ionized; hence, the acidic pK_a reflects protonation of the acid/base (pK_a 6.96), while the alkaline pK_a reflects the ionization of **2** (pK_a 8.4).[25] A similar interpretation of the pK_a's of **1** is not possible because both values are equally distant from the acid−base pK_a; likewise, the basic pK_a of **1** for inhibition (pK_a 7.3) is notably different from its measured pK_a (6.3−6.7).[10,25] Nevertheless, the pH profile for **1** indicates that it optimally interacts with a doubly ionized enzyme. It has long been argued that **1** binds to glucosidases (including almond) as the neutral amine despite the admitted ambiguity in assigning the pK_a's of inhibition.[10,26]

As with the inhibition of Cel5A[20] and other glycosidases[10,24] by iminosugars, the inhibition of *Tm*GH1 with **1** and **2** as a function of pH does not correlate with the pH dependence of k_{cat}/K_M of the enzyme. Optimal inhibition occurs at pH values where the acid−base of the enzyme becomes ionized and catalysis is reduced or absent. Indeed, optimal inhibition of *Tm*GH1 by **2** occurs at a pH value where the enzyme displays greatly reduced activity. The data also emphasize why the literature tends to report inhibitor K_i values at a single pH value, chosen to maximize inhibition constants, rather than at the pH optimum for catalysis. At a minimum, we suggest that the K_i values at both optima should be reported.

Thermodynamics of Binding of 1-Deoxynojirimycin and Isofagomine. Isothermal titration calorimetry was used to dissect the thermodynamic contributions to binding of **1** and **2** to *Tm*GH1. K_d values, at pH 5.8, determined by ITC to be 8 μM and 68 nM for **1** and **2**, respectively, are in reasonable agreement with the corresponding K_i values of 9 μM and 23 nM, determined by kinetic means (Figure 3). In three different buffers and two different pH values (pH 5.8 and 7.0), the binding of both **1** and **2** to *Tm*GH1 is predominantly driven by a large favorable change in enthalpy (ΔH_a), in marked contrast to previous results using van't Hoff analyses ($-\ln K_i$ vs $1/T$) of the sweet almond β-glucosidase, discussed further below. The dependence of ΔH_a on the heat of ionization of the buffer in which the experiment was performed gives a quantitative measure of proton transfer upon binding.[27] Quantitative analysis of ΔH_a in MES and citrate buffers (pH 5.8) gave negative values of n_{H+} of −1.03 (±0.11) for **1** and −0.96 (±0.04) for **2**, consistent with the release of approximately one proton upon

(16) Dale, M. P.; Kopfler, W. P.; Chait, I.; Byers, L. D. *Biochemistry* **1986**, *25*, 2522−2529.
(17) McIntosh, L. P.; Hand, G.; Johnson, P. E.; Joshi, M. D.; Korner, M.; Plesniak, L. A.; Ziser, L.; Wakarchuk, W. W.; Withers, S. G. *Biochemistry* **1996**, *35*, 9958.
(18) MacLeod, A. M.; Tull, D.; Rupitz, K.; Warren, R. A. J.; Withers, S. G. *Biochemistry* **1996**, *35*, 13165.
(19) Vocadlo, D. J.; Wicki, J.; Rupitz, K.; Withers, S. G. *Biochemistry* **2002**, *41*, 9736.
(20) Varrot, A.; Tarling, C. A.; Macdonald, J. M.; Stick, R. V.; Zechel, D. L.; Withers, S. G.; Davies, G. J. *J. Am. Chem. Soc.* **2003**, *125*, 7496−7497.
(21) Fersht, A. *Structure and Mechanism in Protein Science: A guide to enzyme catalysis and protein folding*; W. H. Freeman and Company: New York, 1999.
(22) Lohse, A.; Hardlei, T.; Jensen, A.; Plesner, I. W.; Bols, M. *Biochem. J.* **2000**, *349*, 211−215.
(23) Tanaka, A.; Ito, M.; Hiromi, K. *J. Biochem. (Tokyo)* **1986**, *100*, 1379−1385.
(24) Axamawaty, M. T.; Fleet, G. W.; Hannah, K. A.; Namgoong, S. K.; Sinnott, M. L. *Biochem. J.* **1990**, *266*, 245−249.
(25) Jensen, H. H.; Lyngbye, L.; Bols, M. *Angew. Chem., Int. Ed.* **2001**, *40*, 3447−3449.
(26) Legler, G. *Adv. Carbohydr. Chem. Biochem.* **1990**, *48*, 319−385.
(27) Pierce, M. M.; Raman, C. S.; Nall, B. T. *Methods* **1999**, *19*, 213−221.

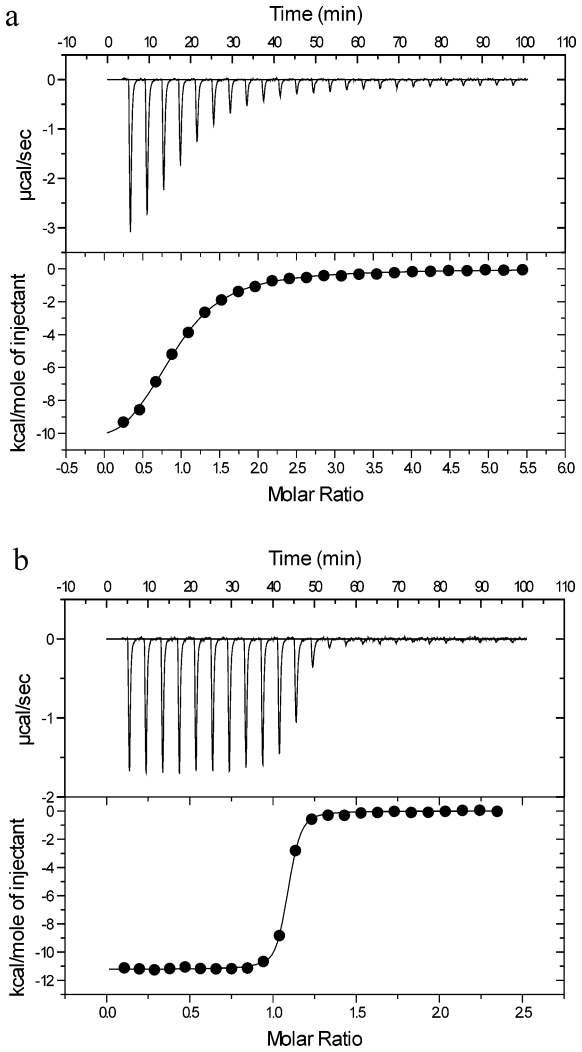

Figure 3. (a) Raw data (top panel) for ITC titrations of *Tm*GH1 β-glucosidase (pH 5.8, 25 °C) with **1** and the curve-fit to a bimolecular binding model (lower panel). (b) ITC data for **2**.

binding either inhibitor. Based on the pH dependence of inhibition and on previous atomic resolution work on the structurally related endocellulase Cel5A in complex with a cellobio-derived form of **2**, the acid−base of *Tm*GH1 is expected to release a proton upon binding protonated **2** at pH 5.8. An indistinguishable scenario is that **1** or **2** first ionizes to a neutral form that binds *Tm*GH1 and is subsequently protonated in the active site by the acid−base. Either situation would lead to the net release of a proton.

ΔH_a values of −7.93 (±0.22) and −6.81 (±0.11) kcal mol^{-1}, in citrate buffer, or, when corrected for the heat of ionization, −8.75 and −7.58 kcal mol^{-1}, are obtained for **1** and **2**, respectively, at the pH optimum of the enzyme (Table 1). A notable dissimilarity in the binding of **1** and **2** to *Tm*GH1 is the difference between the changes in entropy ($T\Delta S_a$) [+3.09 (±0.11) kcal mol^{-1} for **2** as compared to −0.94 (±0.24) kcal mol^{-1} for **1**]. Favorable entropic terms are observed for **2** relative to **1** in the other buffers as well, although the absolute values vary considerably (Table 1). Because the ΔH_a values are relatively similar, it is essentially the large favorable entropy term that makes **2** a better inhibitor than **1**, rather than greater enthalpy, although in both cases binding is dominated by large favorable enthalpies.

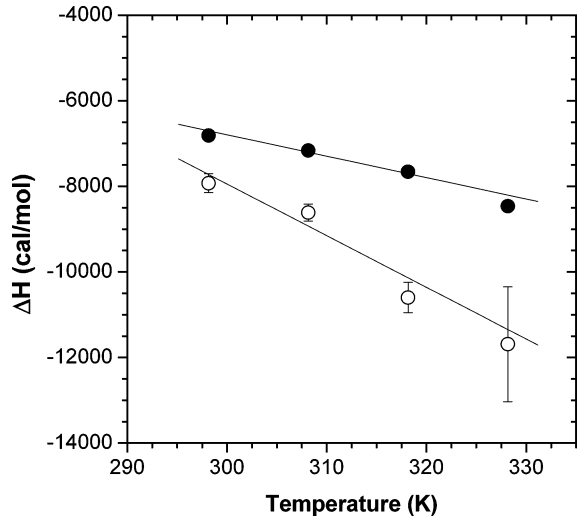

Figure 4. Temperature dependencies of binding enthalpies (ΔH) for the association of **1** (○) and **2** (●) with *Tm*GH1. Solid lines show results of fits by linear regression. Errors bars represent the standard errors of duplicate or triplicate experiments. Where error bars are not visible, the error was within the size of the symbols.

Markedly different heat capacities of association, ΔC_p, are also observed for **1** and **2**, as indicated by the very different temperature dependencies of ΔH_a (Figure 4). Linear regression of these plots gives ΔC_p values of −120.8 (±19.0) cal mol^{-1} K^{-1} for **1** and −50.1 (±3.6) cal mol^{-1} K^{-1} for **2**. ΔC_p is often considered to be a measure of solvent rearrangement in a molecular interaction;[28] large negative values are thought to represent solvent release from apolar surfaces. However, this view is complicated by the observation of negative contributions to ΔC_p from water molecules that become ordered at newly formed molecular interfaces (see below).[29] Nevertheless, the discrepancy between the ΔC_p's further highlights the differing thermodynamic signatures of interaction of **1** and **2** with *Tm*GH1.

An explanation for the differences in the binding thermodynamics is offered by considering the relative differences in the thermodynamic parameters for **1** and **2**: $\Delta\Delta H_a$ [$=\Delta H_a$ (**1**) − ΔH_a (**2**) = −1.17 kcal mol^{-1} (corrected for heat of ionization)], $T\Delta\Delta S_a$ ($=T\Delta S_a$ (**1**) − $T\Delta S_a$ (**2**) = −4.03 kcal mol^{-1}), and $\Delta\Delta C_p$ ($=\Delta C_p$ (**1**) − ΔC_p (**2**) = −70.7 (±31.3) cal mol^{-1} K^{-1}). Favorable contributions to enthalpy, unfavorable contributions to entropy, and negative contributions to heat capacity are reminiscent of waters becoming ordered at a molecular interface.[29,30] Estimates suggest that each water molecule that is ordered at an interface can contribute −0.5 to −3.0 kcal mol^{-1} to ΔH_a,[29,30] but this also has a corresponding negative effect on $T\Delta S_a$.[30,31] Furthermore, contributions of −48 to −60 cal mol^{-1} K^{-1} water^{-1} to ΔC_p have been estimated for the ordering of a water molecule.[29,32] On the basis of these values, our results would appear to be consistent with the binding of **1** incorporating approximately 1−3 more water molecules at the molecular interface relative to the binding of **2**. Indeed, a single ordered

(28) Chervenak, M. C.; Toone, E. J. *Biochemistry* **1995**, *34*, 5685−5695.
(29) Holdgate, G. A.; Tunnicliffe, A.; Ward, W. H.; Weston, S. A.; Rosenbrock, G.; Barth, P. T.; Taylor, I. W.; Pauptit, R. A.; Timms, D. *Biochemistry* **1997**, *36*, 9663−9673.
(30) Clarke, C.; Woods, R. J.; Gluska, J.; Cooper, A.; Nutley, M. A.; Boons, G. J. *J. Am. Chem. Soc.* **2001**, *123*, 12238−12247.
(31) Dunitz, J. D. *Science* **1994**, *264*, 670.
(32) Habermann, S. M.; Murphy, K. P. *Protein Sci.* **1996**, *5*, 1229−1239.

Table 1. Thermodynamic Parameters of *Thermotoga maritima* GH-1 β-Glucosidase Binding to 1-Deoxynojirimycin and Isofagomine

	1-deoxynojirimycin (**1**)			(+)-isofagomine (**2**)		
	K-Phos[a]	MES[b]	citrate[c]	K-Phos[a]	MES[b]	citrate[c]
K_a ($\times 10^6$ M^{-1})	0.21 ($\pm$0.01)	0.14 ($\pm$0.01)	0.11 ($\pm$0.01)	51.45 ($\pm$21.42)	29.20 ($\pm$0.85)	14.65 ($\pm$0.35)
ΔG_a (kcal/mol)	$-$7.96 ($\pm$0.00)	$-$7.09 ($\pm$0.03)	$-$6.99 ($\pm$0.00)	$-$10.63 ($\pm$0.26)	$-$11.15 ($\pm$0.23)	$-$9.90 ($\pm$0.01)
ΔH_a (kcal/mol)	$-$11.29 ($\pm$0.01)	$-$12.55 ($\pm$0.60)	$-$7.93 ($\pm$0.22)	$-$9.68 ($\pm$0.22)	$-$10.32 ($\pm$0.02)	$-$6.81 ($\pm$0.11)
$T\Delta S_a$ (kcal/mol)	$-$3.93 ($\pm$0.01)	$-$5.46 ($\pm$0.60)	$-$0.94 ($\pm$0.24)	0.95 ($\pm$0.26)	$-$0.83 ($\pm$0.23)	3.09 ($\pm$0.11)
n	0.98 ($\pm$0.01)	0.85 ($\pm$0.01)	1.03 ($\pm$0.00)	1.01 ($\pm$0.01)	1.07 ($\pm$0.04)	1.07 ($\pm$0.04)

[a] 100 mM potassium phosphate, pH 7.0. [b] 100 mM MES, pH 5.8. [c] 100 mM sodium citrate, pH 5.8.

water molecule is observed to hydrogen bond to the N5 of **1** in the active site of *Tm*GH1 (see crystallography below), similar to that observed in the xylanase, Cex.[33] This water is not present in the crystal structure of *Tm*GH1 in complex with **2**. Although one may predict that incorporation of features into **1** that displace these water molecules would improve the entropic term,[29] and hence the affinity of **1**, *N*-methyl and *N*,*N*-dimethyl derivatives of **1** are known to be weaker inhibitors of almond β-glucosidase.[26,34] The reason for this requires further investigation. No information is available about the degree of solvation of **1** and **2** in free solution, and consequently interpretations based upon observation of one-half of an equilibrium must be treated with due caution. Indeed, it is possible that **2** is more conformationally restrained in bulk solution and therefore does not incur the same entropic penalty upon binding as was observed for **1**. Likewise, different thermodynamic signatures for **1** and **2** can be expected at the temperature optimum of *Tm*GH1 ($\sim$80 °C) as the thermodynamic parameters are clearly temperature dependent.

Reassessment of the Binding of 1 and 2 to Sweet Almond β-Glucosidase. Given the stark contrast between the calorimetric data presented here for *Tm*GH1 and the values obtained by van't Hoff methods on the related sweet almond β-glucosidase (also from family GH-1) which instead suggest that binding of racemic **2** is driven by entropy, we performed calorimetric measurements on the sweet almond enzyme under the conditions used for van't Hoff work (phosphate buffer, pH 7.0). It is immediately and unambiguously apparent, as shown by the negative power deflections of the ITC data (Figure 5), that the binding of both **1** and (+)-**2** to almond β-glucosidase is exothermic and therefore enthalpically favorable. At 25 °C, the interaction of **1** with almond β-glucosidase is dominated by a favorable ΔH_a with a minor but favorable contribution to ΔS_a (Table 2). At 35 °C, the interaction remains enthalpically driven but is partially offset by an unfavorable contribution to ΔS_a. As observed for *Tm*GH1, the calculated ΔS_a values for (+)-**2** at both temperatures are markedly favorable (Table 2), but binding is nevertheless dominated by ΔH_a. Furthermore, non-stoichiometric titration of the theoretical number of active sites was observed with **1** and (+)-**2** ($n = 0.35-0.38$), confirming that commercial almond β-glucosidase preparations are largely inactive, consistent with values obtained by others.[15] It is evident that the continued use of sweet almond β-glucosidase as the "workhorse" of β-glycosidase inhibition is questionable.

It is noteworthy that the calorimetric thermodynamic parameters for **1** binding to almond β-glucosidase approximate those determined by a simple van't Hoff analysis. However, the

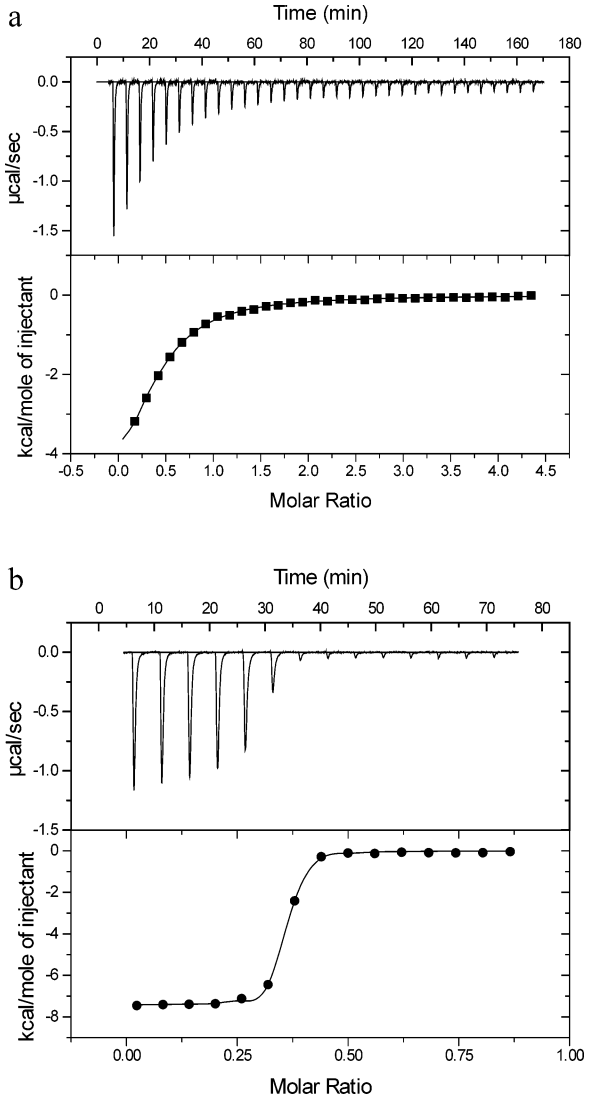

Figure 5. (a) Raw data (top panel) for ITC titrations of sweet almond β-glucosidase (pH 7.0, 25 °C) with **1** and the curve-fit to a bimolecular binding model (lower panel). (b) ITC data for **2**. Note that stoichiometric titration is not observed due to the substantial inactivity of almond β-glucosidase preparations.

calorimetric and van't Hoff thermodynamic parameters for (+)-**2** are profoundly different. Discrepancies between van't Hoff and calorimetric data are not without precedent,[35] and their cause remains unclear.[36] While in some cases these differences can be attributed to experimental error,[36] there are notable cases in

(33) Notenboom, V.; Williams, S. J.; Hoos, R.; Withers, S. G.; Rose, D. R. *Biochemistry* **2000**, *39*, 11553−11563.
(34) Li, Y. K.; Byers, L. D. *Biochim. Biophys. Acta* **1989**, *999*, 227−232.
(35) (a) Faergeman, N. J.; Sigurskjold, B. W.; Kragelund, B. B.; Anderson, K. V.; Knudsen, J. *Biochemistry* **1996**, *35*, 14118−14126. (b) Naghibi, H.; Tamura, A.; Sturtevant, J. M. *Proc. Natl. Acad. Sci. U.S.A.* **1995**, *92*, 5597−5599.
(36) Horn, J. R.; Russell, D.; Lewis, E. A.; Murphy, K. P. *Biochemistry* **2001**, *40*, 1774−1778.

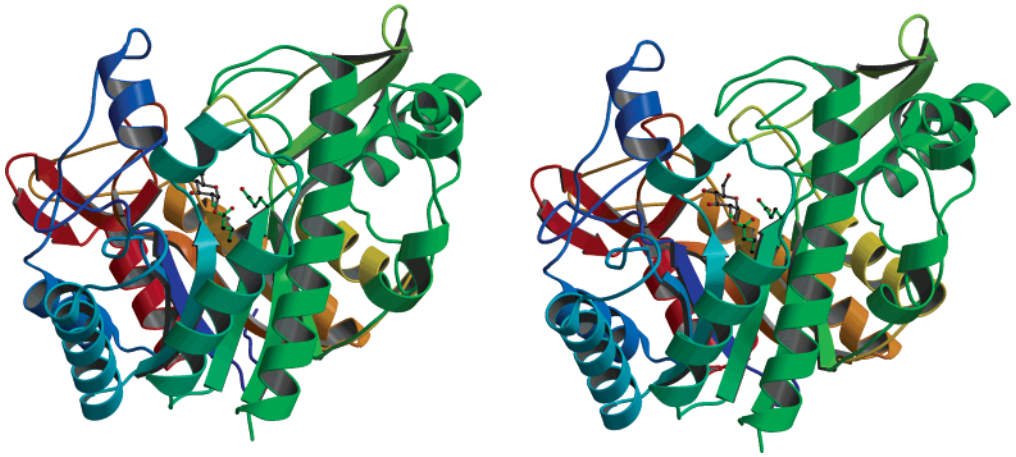

Figure 6. 3-D structure of *Tm*GH1 determined by X-ray crystallography, drawn with BOBSCRIPT[59] in divergent ("wall-eyed") stereo. The covalent 2-F glucosyl-enzyme intermediate, along with acid/base and nucleophile Glu166 and Glu315, are shown in the "ball-and-stick" representation.

Table 2. Thermodynamic Parameters of Almond β-Glucosidase Binding to 1-Deoxynojirimycin and Isofagomine in 100 mM Potassium Phosphate, pH 7.0

	1-deoxynojirimycin (**1**)		(+)-isofagomine (**2**)	
	25 °C	35 °C	25 °C	35 °C
K_a ($\times 10^6$ M^{-1})	0.043 (±0.001)	0.028 (±0.001)	17.40 (±2.33)	36.50 (±3.40)
ΔG_a (kcal/mol)	−6.39 (±0.02)	−6.34 (±0.02)	−10.10 (±0.10)	−10.80 (±0.08)
ΔH_a (kcal/mol)	−6.32 (±0.19)	−8.69 (±0.39)	−7.41 (±0.02)	−8.26 (±0.05)
$T\Delta S_a$ (kcal/mol)	0.09 (±0.18)	−2.35 (±0.38)	2.68 (±0.8)	2.54 (±0.09)
n	0.38 (±0.01)	0.37 (±0.02)	0.36 (±0.02)	0.35 (±0.01)

which the calorimetric and van't Hoff values contrast sharply.[37,38] This study appears to be another notable case. It is well known that the neglect of ΔC_p in the van't Hoff analysis, which is significant for the binding of **1** and (+)-**2**, can result in relatively large errors in the calculated thermodynamic parameters.[36] Also of concern is the ionization behavior of (+)-**2** as well as conformational changes in almond β-glucosidase that may occur upon inhibitor binding.[23,26] Such equilibria linked to ligand binding have been proposed to obscure correct interpretation of van't Hoff analysis.[36,37]

Given the unambiguous release of heat upon binding of **1** and **2** to the sweet almond β-glucosidase, plus essentially identical results obtained for *Tm*GH1, we conclude that on both of these systems, in contrast to previous reports, the binding of **1** and **2** is dominated by favorable enthalpy. The greater prowess of **2** as compared to **1** is, however, due to its substantially more favorable entropy. To shed some light upon these unusual phenomena, the 3-D structure of *Tm*GH1 was determined in native and trapped 2-fluoro glycosyl-enzyme intermediate forms and in complex with both **1** and (+)-**2**.

The 3-D Structure of *Tm*GH1. The 3-D structure of native *Tm*GH1 was determined at a resolution of 2.1 Å using synchrotron data (Table 3). The structure forms a classical $(\alpha/\beta)_8$ barrel with the "antiprotonating[2b]" acid/base (Glu 166) on strand 4 and nucleophile (Glu351) on strand 7 as expected for this "GH-A clan"[39] (Figure 6). Almost the whole of the chain can be traced for both molecules of the asymmetric unit of the $P2_12_12_1$ crystal form, although residues 213, 233, and 305−306 show differing levels of mobility in the various structures and have been omitted from some deposited models. Many features of *Tm*GH1 are as described previously for other enzymes from the sequence family. The active site is located some 15−20 Å deep in a pocket with the "exo" nature of this glycosidase governed by Gln20, Glu405, and Trp406 around the −1 binding site. The structure of the covalent 2-fluoro-glycosyl-enzyme intermediate was determined at 2.15 Å (Figures 6, 7a), confirming that Glu351 is the nucleophile in the reaction. The covalent-intermediate lies in a classical $^4C_1$ conformation with a slight rotation of the nucleophile to avoid an unfavorable clash of the 2-fluoro group with the nucleophile carbonyl moiety, as observed on other systems.

The structure of *Tm*GH1 with **1**, at 2.1 Å resolution, reveals binding in the −1 site as expected. The 2-hydroxyl (2-OH) of **1** hydrogen bonds to both the nucleophile and the Asn165 (the signature interactions of clan GH-A[39]); 3-OH bonds to His121, Trp406, and the side-chain carbonyl of Gln20; 4-OH bonds to the amide of Gln20, Trp398, and the carboxylate of Glu405; and 6-OH bonds to the side chain of Glu405 (Figures 7b, 8a). All hydrogen bond distances are around 2.8−3.1 Å (±0.2 Å). Maximum-likelihood refinement with no restraint on pyranoside torsion angles causes distortion of **1** from $^4C_1$ with C1 slightly displaced upward (toward $^4H_3$ and $^1S_3$) allowing the nucleophile to interact with both O2 and N5 of **1**. Given that such distortion has not been observed on other glycosidase structures with derivatives of **1**,[33,40] it is unclear whether this motion reflects a genuine distortion driven by van der Waals' contacts with the nucleophile and H-bond optimization or is a consequence of medium resolution data. The closest approach of the carboxylate oxygen of the nucleophile to C1 is approximately 3 Å. Of particular note are the interactions of the N5 nitrogen. This atom

(37) Sigurskjold, B. W.; Bundle, D. R. *J. Biol. Chem.* **1992**, *267*, 8371−8376.
(38) Wang, X.; Pielak, G. J. *Biochemistry* **1999**, *38*, 16876−16881.
(39) Henrissat, B.; Callebaut, I.; Fabrega, S.; Lehn, P.; Mornon, J.-P.; Davies, G. *Proc. Natl. Acad. Sci. U.S.A.* **1995**, *92*, 7090−7094.
(40) The 1Å structure of *S. lividans* Xyn10A has been refined in complex with a xylobio derivative of **1**, Gloster, et al., unpublished.

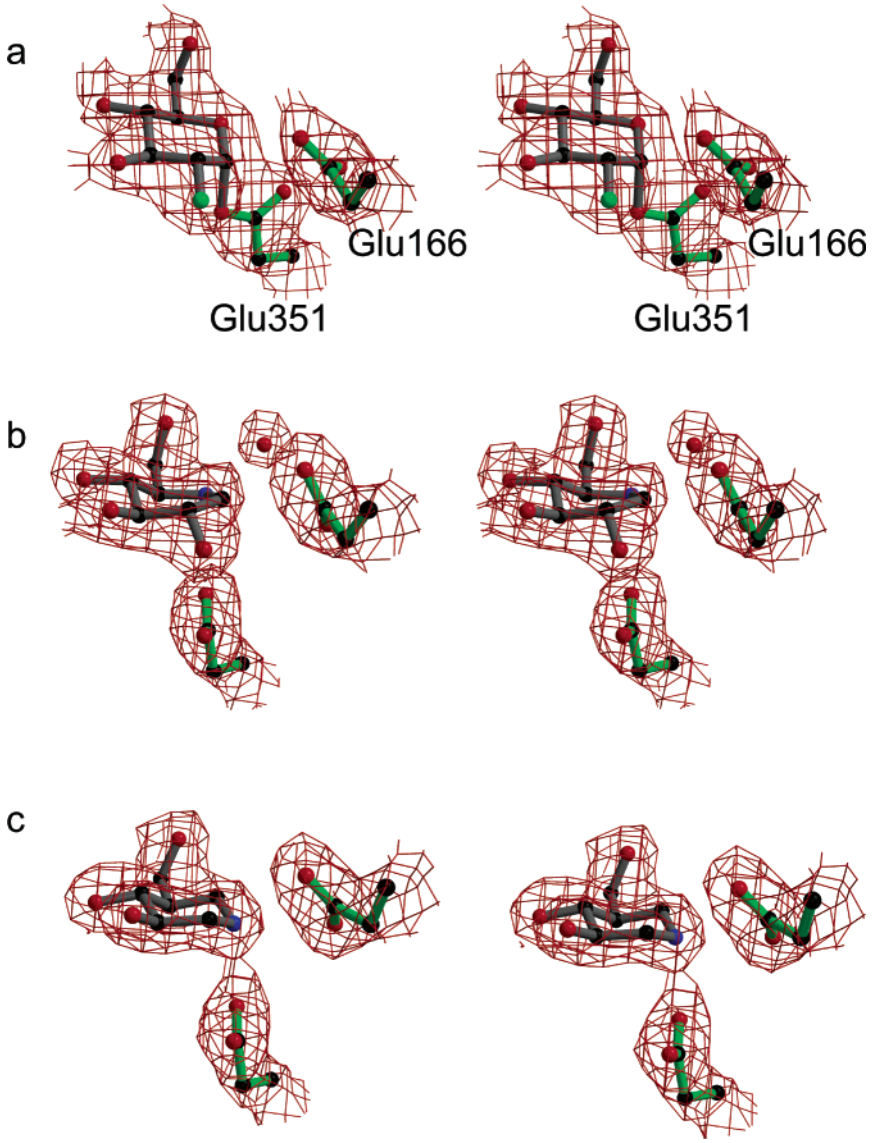

Figure 7. Observed electron density for the binding of (a) the 2-fluoro glucosyl-enzyme intermediate (b) **1** and (c) **2** to *Tm*GH1. The figures shown are drawn with BOBSCRIPT[59] with maximum-likelihood/σ_A weighted[60] $2F_{obs} - F_{calc}$ density contoured at 1σ ($\sim$0.25 e/Å^3) in divergent stereo.

makes one clear hydrogen bond to a solvent water molecule. A second water molecule is not evident from the electron density; indeed Tyr295 lies approximately 3.6 Å "below" N5 and thus blocks the potential interaction with the lone pair (or proton) of N5. In this way, *Tm*GH1 would appear to be different in its N5 interactions with family 10 xylanases[33,40] where two water molecules coordinate N5.

The binding of **2** to *Tm*GH1 at a resolution of 2.15 Å reveals similar interactions at the 3-OH, 4-OH, and 6-OH positions (Figures 7c, 8b) and adopts a relaxed $^4C_1$ conformation. Unlike **1**, however, the interaction of **2** with *Tm*GH1 does not involve ordered water molecules. N1 lies 2.6 Å from the carboxylate OE1 oxygen of the nucleophile Glu351, suggesting a tight electrostatic interaction. Likewise, the acid/base catalyst also appears to form a Coulombic interaction with N1 (3.1 Å). Although the resolution of these structures does not allow direct observation of the ionization state of **2** and the catalytic apparatus, an atomic resolution structure for Cel5A with the cellobio-derivative of **2**[20] provides precedent for the inhibitor binding to a doubly ionized enzyme. This clamping mode of binding N1 between the nucleophile and the acid/base has also been observed on a β-*N*-acetylhexosaminidase with a derivative of **2**.[41]

Transition-State Mimics or Fortuitous Binders? By definition, a "transition-state mimic" is never perfect and will not capture all of the binding energy available in an enzyme active site for the reaction transition state. In assessing a transition-state analogue, one is forced to determine what enzyme-inhibitor interactions are relevant to transition-state binding, as well as what interactions are absent. The three-dimensional structures of inhibitor complexes can identify interactions with enzyme active site residues, and these can be compared to what is known about transition-state stabilization from biochemical studies. The correlation of K_i with k_{cat}/K_M in pH profiles or linear free energy relationships (LFERs),[1] as well as the thermodynamic parameters for binding, offer an objective means of grading a transition-state mimic.[4,5]

Certainly **1** and **2** achieve some semblance of the glucosidase

(41) Mark, B. L.; Vocadlo, D. J.; Zhao, D. L.; Knapp, S.; Withers, S. G.; James, M. N. G. *J. Biol. Chem.* **2001**, *276*, 42131−42137.

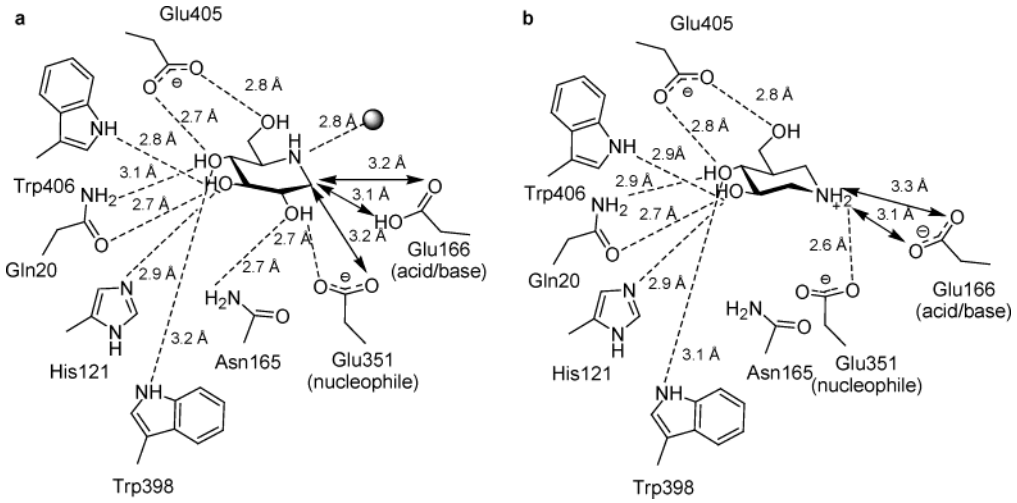

Figure 8. A scheme of **1** and **2** bound to *Tm*GH1. The protonated form of **2** is based upon pH profiles and the published atomic resolution structure of a related enzyme,[20] while **1** is shown unprotonated as there is currently no unambiguous proof as to its ionization state; the most likely binding form at pH 5.8 would be with a partially protonated form of **1**.

transition state as both have been successfully used as haptens to elicit catalytic antibodies that exhibit glucosidase activity.[42,43] These activities, not surprisingly, are very low relative to natural enzymes. Likewise, both **1** and **2** bind to β-glucosidases with large and favorable enthalpies, as expected for transition-state analogues.[5] However, a deficiency with **1** and **2** as transition-state mimics is the absence of constraint into a $^4H_3$ conformation (any distortion must necessarily pay an energetic cost). **2** is also compromised by the absence of a 2-hydroxyl and thus is unable to form known key catalytic interactions with the nucleophile and Asn165.[44] It is known that the substrate 2-OH contributes at least 4.5 kcal mol^{-1} to transition-state stabilization by family 1 β-glucosidases[45] (and up to 10 Kcal mol^{-1} in other glycosidases[46]) whereas the remaining hydroxyl groups contribute 1−2 kcal mol^{-1}. However, an analogue of **2** bearing a 2-hydroxyl, noeuromycin, is not a significantly better inhibitor of retaining β-glycosidases, including almond (although, interestingly, noeuromycin is a substantially better inhibitor of α-glycosidases).[44] This is indicative of a lack of transition-state character, as modifications of the analogue do not affect K_i in a way that correlates with changes in the k_{cat}/K_M value upon an equivalent change in a substrate.[1] Likewise, no correlation between K_i and k_{cat}/K_M in a LFER was observed with a family 1 β-glucosidase and **1**.[9] Thus, the affinities of **1** and **2** would appear to stem predominantly from interactions that are not equivalent to those in the β-glucosidase transition state. One possibility with **2** is the electrostatic interaction of the acid/base with the "anomeric" N1. This interaction dominates the pH dependence of K_i, rather than the nucleophile, as had been assumed previously.[12] The consequence of this interaction is that **2** binds optimally to a doubly ionized and largely inactive enzyme as shown by the pH profile in Figure 1, indicating that this interaction is not pK_a optimized, or perhaps catalytically irrelevant.

Although **2** is thought to be a better mimic than **1** of the β-glucosidase transition state, the fact that the superior inhibition of **2** is derived solely from entropy, a thermodynamic term not observed to dominate transition-state binding by enzymes, casts doubt on this view. Likewise, the notably weaker temperature dependence of ΔH_a for **2** relative to **1** is also at odds with the strong temperature dependence of $\Delta H^{\ddagger}$ observed for enzyme-catalyzed reactions, as well as ΔH_a of "good" transition-state mimics.[4,5] Intriguingly, favorable (even dominant) $T\Delta S_a$ values and unusually low ΔH_a values were observed in a calorimetric study of the binding of phosphonate transition-state analogues to an esterase catalytic antibody.[47] This was attributed to desolvation of complementary charges on the transition-state analogues and antibody active site residues upon binding without forming equally compensating electrostatic interactions. In this scenario, desolvation of the charged groups contributes favorably to $T\Delta S_a$, but the resulting electrostatic interactions fail to contribute favorably to ΔH_a. Nonoptimized electrostatic interactions may well be the reason for the poor catalytic activity of the antibody. An analogous explanation for the thermodynamic parameters of positively charged **2** is also possible. As more transition-state analogues are characterized by calorimetry in parallel with correlations between K_i and k_{cat}/K_M, a better understanding of what is an ideal thermodynamic signature for a transition-state analogue will emerge.

Materials and Methods

Cloning, Expression, and Purification of *Tm*GH1. The *Thermotoga maritima* β-glucosidase (*Tm*GH1) gene, based upon that reported in Genbank entry X74163, was obtained by PCR on *Thermotoga maritima* genomic DNA (American Type Culture Collection ATCC). An inconsistency we cannot resolve is that this gene is not reported in the deposited *T. maritima* genome sequence despite our amplification from DNA supplied from the ATCC.

The primers used were 5′-AGCCATATGGCTAGCAACGTGAAA-AAGTTCCCTGAAGGA-3′ (forward primer) and 5′-AGTGCGGC-CGCAAGCTTTAGTCTTCCAGACCGTTGTTTTTCAACAC-3′ (reverse primer). *Nhe*I and *Hind*III restriction sites are underlined. The PCR product was cloned into pET-28a (Novagen) via the *Nhe*I and *Hind*III sites yielding a *Tm*GH1 construct with a 6 × His sequence at

(42) Yu, J.; Choi, S. Y.; Moon, K.-D.; Chung, H.-H.; Youn, H. J.; Jeong, S.; Park, H.; Schultz, P. G. *Proc. Natl. Acad. Sci. U.S.A.* **1998**, *95*, 2880−2884.
(43) Goud, G. N.; Artsaenko, O.; Bols, M.; Sierks, M. *Biotechnol. Prog.* **2001**, *17*, 197−202.
(44) Liu, H.; Liang, X.; Søhoel, H.; Bülow, A.; Bols, M. *J. Am. Chem. Soc.* **2001**, *123*, 5116.
(45) Namchuk, M. N.; Withers, S. G. *Biochemistry* **1995**, *34*, 16194−16202.
(46) White, A.; Tull, D.; Johns, K.; Gilkes, N. R.; Withers, S. G.; Rose, D. R. *Nat. Struct. Biol.* **1996**, *3*, 149−154.
(47) Wade, H.; Scanlan, T. S. *ChemBioChem* **2003**, *4*, 531−540.

the N-terminus, herein called pET-28a-*Tm*GH1-His$_6$. Heat shock competent *E. coli* cells (BL21) were transformed with pET-28a-*Tm*GH1-His$_6$ and selected on LB-agarose plates containing 50 μg/mL kanamycin. Transformed cells were grown in TYP media (50 μg/mL kanamycin) at 37 °C (140 rpm) to a high OD_{600} of 3, induced with 0.5 mM IPTG, and allowed to grow overnight. The cells were harvested by centrifugation (8000 rpm, 10 min), resuspended in 10 mM imidazole, 300 mM NaCl, pH 7, and then lysed by sonication. Benzonuclease (Novagen) was added to digest the DNA. After centrifugation (15 000 rpm, 20 min), the supernatant was heated to 75 °C for 20 min. The resulting precipitate was removed by centrifugation (15 000 rpm, 20 min), and the supernatant was applied to a Ni^{2+} agarose column (Novagen). *Tm*GH1-His$_6$ was eluted using a step gradient of imidazole, affording >95% pure protein as judged by SDS-PAGE. The yield of *Tm*GH1-His$_6$ was approximately 15 mg L^{-1}.

A *Tm*GH1 construct lacking a His$_6$ tag was obtained by subcloning the *Nde*I/*Hind*III fragment derived from pET-28a-*Tm*GH1-His$_6$ into the *Nde*I/*Hind*III sites of pET-22b (Novagen), yielding the plasmid pET-22b-*Tm*GH1. Heat shock competent *E. coli* BL21 cells were transformed with pET-22b-*Tm*GH1 and selected on LB-agarose plates containing 100 μg/mL ampicillin. Transformed cells were grown in LB media (100 μg/mL ampicillin) to an OD 600 nm of ~0.6, induced with 0.5 mM IPTG, and then allowed to grow overnight. Extra ampicillin was added after 8 h (50 μg/mL). The cells were collected by centrifugation, resuspended in 20 mM BisTris propane, pH 6.8, and lysed by sonication. Benzonuclease was added to digest the DNA. Following centrifugation, the resulting supernatant was heated to 75 °C for 20 min. The precipitate was removed by centrifugation, and a concentrated ammonium sulfate solution (pH 7) was added to the supernatant to achieve a final concentration of 1.0 M. The supernatant was loaded onto a Phenyl Sepharose High Performance column (Pharmacia), washed with 5 column volumes of 1.0 M ammonium sulfate, and then eluted with a linear gradient to 0 M ammonium sulfate, 20 mM BisTris Propane, over 10 column volumes. The *Tm*GH1 fraction was pooled, concentrated and dialyzed into 20 mM BisTris Propane, pH 6.8, and then loaded onto a Sepharose Q column (Pharmacia). After the column was washed with 5 column volumes of 20 mM BisTris Propane, *Tm*GH1 was eluted using a linear gradient to 500 mM NaCl. SDS-PAGE analysis indicated single band purity for the pooled fractions. MALDI-MS analysis (sinapinic acid matrix) gave masses of 51 751 and 53 941 Da for *Tm*GH1 and *Tm*GH1-His$_6$, respectively.

Active Site Labeling and ESI-MS Analysis. *Tm*GH1 and *Tm*GH1-His$_6$ (10−65 μM) were incubated with an excess of 2,4-dinitrophenyl 2-deoxy-2-fluoro-β-D-glucopyranoside (180 μM) in 100 mM sodium phosphate (pH 7.0) at room temperature for 3 h. Volumes of enzyme and buffer were determined by mass on an analytical balance. The 2,4-dinitrophenol released was quantified spectrophotometrically at 400 nm using an extinction coefficient of 10 910 M^{-1} cm^{-1}.[48] The absorbance values were corrected by a blank solution containing only inactivator, incubated under the same conditions. An assay of activity after 3 h using 4-nitrophenyl β-D-glucopyranoside indicated >99.9% of the enzyme had been inactivated. The concentration of the enzyme stock solutions was determined by absorbance at 280 nm using the extinction coefficient 118 630 M^{-1} cm^{-1} (calculated from the amino acid sequence[49]). From these data, *n* values of 0.826 (±0.004) and 0.835 (±0.007) were calculated for *Tm*GH1-His$_6$ and *Tm*GH1, respectively. The 2,4-dinitrophenolate extinction coefficient was also determined under our experimental conditions (according to ref 48), affording a value of 8890 M^{-1} cm^{-1}. Using this coefficient, *n* values of 1.014 (±0.004) and 1.025 (±0.007) were calculated for *Tm*GH1-His$_6$ and *Tm*GH1, respectively. ESI-MS analysis (performed by Shouming He, Department of Chemistry, University of British Columbia) gave masses of 51 750 and 51 584 Da for labeled and unlabeled *Tm*GH1, respectively, corresponding to a mass difference of 166 Da (100% conversion to the labeled enzyme was observed).

Steady-State Kinetics. Activity was monitored spectrophotometrically using 2,4-dinitrophenyl β-D-glucopyranoside as a substrate. Solutions of substrate in 100 mM sodium phosphate, 1 mg mL^{-1} BSA, pH 7.0 (total volume of 750 μL), were equilibrated at 25 °C. Reaction was initiated by the addition of a small volume of enzyme (2.5−5 μL), and 2,4-dinitrophenol release was monitored continuously at 400 nm (ϵ_{400} = 8890 M^{-1} cm^{-1}). Concentrations of substrate ranged from 0.01 to 2.1 mM, and enzyme concentrations ranged from 10 to 20 nM. The Michaelis Menten equation was fit to the data using GraFit.[50] Virtually identical kinetic parameters were calculated for *Tm*GH1-His$_6$ (k_{cat} = 42 ± 1 s^{-1}, K_M = 0.41 ± 0.03 mM) and for *Tm*GH1 (k_{cat} = 42 ± 1 s^{-1}, K_M = 0.30 ± 0.02 mM).

pH Dependence of k_{cat}/K_M. Approximate values of k_{cat}/K_M as a function of pH for the reaction of *Tm*GH1 with 2,4-dinitrophenyl β-D-glucopyranoside were calculated from first-order rate curves generated at low substrate concentrations ([S] ≪ K_m). Assays were performed at 25 °C and consisted of 12.6 μM substrate, 86 mM buffer, and 1 mg mL^{-1} BSA (total volume 750 μL). The reaction was initiated by addition of a small volume of *Tm*GH1 (5−10 μL) to afford a final concentration of 33−110 nM enzyme. The following buffers were used for each pH range: 86 mM citrate, pH 4−6; 86 mM sodium phosphate, pH 6−8. Overlapping data from citrate and phosphate buffers, as well as halving the concentration of buffer, indicated no significant buffer effects on rates. BSA was omitted below pH 5 due to precipitation in this range. *Tm*GH1 was stable at all pH values within the time range of the assay (10−20 min). 2,4-Dinitrophenol release was monitored continuously at 400 nm for at least 5 half-lives (10−20 min), and the resulting time course was fit to a first-order rate equation (eq 1) using GraFit. The rate constant calculated for the curve ($k = V_{max}/K_M$), adjusted for the concentration of enzyme, affords an approximate value for k_{cat}/K_M. The data were fit with a bell ionization curve (eq 2) using GraFit to determine the pK_a values. Identical buffer solutions were used for the pH dependence of $1/K_i$ (described below).

$$A_{400}^{\,t} = A_{400}^{\,0}(1 - e^{(-kt)}) + \text{offset} \tag{1}$$

$$k_{cat}/K_m \quad \text{or} \quad 1/K_i = \frac{\text{limit} \times 10^{(pH-pKa1)}}{10^{(2\times pH-pKa1-pKa2)} + 10^{(pH-pKa1)} + 1} \tag{2}$$

pH Dependence of $1/K_i$ for 1-Deoxynojirimicin and Isofagomine. K_i values for **1** and **2** were determined at low substrate concentrations ([S] ≪ K_m) in which case the fractional decrease in activity observed in the presence of inhibitor (i) is given by eq 3.[10,51]

$$\frac{v_i}{v_0} = \frac{K_i}{K_i + [I]} \tag{3}$$

In the case of **1**, values of V_{max}/K_m were determined from pseudo-first-order rate curves in the presence and absence of inhibitor. Inhibition assays contained 15 μM 2,4-dinitrophenyl β-D-glucopyranoside, 1 mg mL^{-1} BSA (except below pH 5), and 89 mM buffer. The concentration of **1** was typically 1−10 times the final K_i value. *Tm*GH1 concentrations ranged from 35 to 270 nM. Values of K_i are the average of duplicate or triplicate measurements of $(V_{max}/K_M)_i$ and $(V_{max}/K_M)_0$. The dependence $1/K_i$ versus pH was fit to eq 2 with GraFit.

Slow-onset inhibition was observed with **2** at all pH values (Figure 2). This behavior prevented determination of K_i under pseudo-first-order rate conditions as described for **1**. Rather, K_i values for **2** were determined under steady-state conditions at low substrate concentrations ([S] ≪ K_m) from ratios of v_i and v_o. Assays contained 10 μM 2,4-dinitrophenyl β-D-glucopyranoside, 1 mg mL^{-1} BSA (except below

(48) Kempton, J. B.; Withers, S. G. *Biochemistry* **1992**, *31*, 9961−9969.
(49) Gill, S. C.; von Hippel, P. H. *Anal. Biochem.* **1989**, *182*, 319.
(50) Leatherbarrow, R. J.; 4.014 ed.; Erithacus Software, Ltd.: London, 2001.
(51) Snider, M. J.; Wolfenden, R. *Biochemistry* **2001**, *40*, 11364−11371.

Table 3. X-ray Data and Structure Quality Statistics for the *Thermotoga maritima* Family 1 β-Glucosidase and Its Ligand Complexes

	native	2-FGlc	**1**	**2**
		Data		
resolution (Å)	20−2.10 (2.17−2.10)	20−2.15 (2.2−2.15)	20−2.15 (2.2−2.15)	20−2.15 (2.2−2.15)
R_{merge}	0.069 (0.39)	0.057 (0.40)	0.051 (0.37)	0.056 (0.37)
$I/\sigma I$	19.7 (3.4)	25 (5.1)	25 (3.9)	23 (4.2)
completeness (%)	99.3 (98.1)	100 (100)	99.5 (98.9)	99.2 (98.9)
multiplicity	4.0 (3.6)	5.4 (5.4)	3.7 (3.4)	4.3 (4.3)
beamline	ESRF, ID14-4	ESRF, ID14-2	ESRF, ID14-4	ESRF, ID14-2
		Structure		
rms bonds (Å)	0.010	0.018	0.015	0.015
rms angles (deg)	1.17	1.62	1.27	1.43
R_{cryst}	0.21	0.20	0.19	0.20
R_{free}	0.27	0.25	0.23	0.26
PDB code	1od0	1oin	1oim	1oif

pH 5), and 89 mM buffer. Concentrations of **2** typically varied from 2 to 10 times the final K_i value. Reaction was initiated with the addition of *Tm*GH1 to afford 2.3−4.6 nM enzyme. Rates measured with inhibitor were obtained in the linear region following slow-onset. Final K_i values are the average of duplicate or triplicate independent measurements of v_i and v_o. The dependence $1/K_i$ versus pH was fit with eq 2 using GraFit.

Isothermal Titration Calorimetry. *Tm*GH1 was dialyzed extensively into 100 mM potassium phosphate, pH 7.0, 100 mM MES, pH 5.8, or 100 mM sodium citrate, pH 5.8, using a stirred ultrafiltration cell (Amicon) and a 10 kDa cutoff polyether sulfone membrane (Millipore). Samples for use in ITC were diluted to appropriate concentrations in dialysate buffer saved from the ultrafiltration step. Protein concentration was determined spectrophotometrically, as described above. Chromatographically pure almond β-glucosidase containing 99% protein (Lot 58H4074) was obtained from Sigma (St. Louis, MO). Samples for ITC were prepared by weight in 50 mM potassium phosphate buffer, pH 7.0. The protein concentration was determined using the extinction coefficient $\epsilon_{280} = 103\,000$ (±8000) calculated from the average of theoretical ϵ_{280} values of 10 randomly chosen family 1 glycosidases.[49] All samples were filtered with 0.2 μm cutoff filters (Sartorius) and extensively degassed with stirring prior to use.

Isothermal titration calorimetry (ITC) was performed using a MCS ITC (MicroCal, Inc., Northampton, MA). Inhibitor samples were prepared by weight in buffer saved from the dialysis of *Tm*GH1 or in the same 50 mM potassium phosphate buffer, pH 7.0, as that in which the almond β-glucosidase was prepared. Inhibitor samples were filtered and degassed before use. Titrations were performed by injecting 5 or 10 μL aliquots of **1** (3000 μM) or **2** (485 μM) solution into the ITC sample cell (volume = 1.35 mL) containing *Tm*GH1 or almond β-glucosidase. C values [$C = K_a \times M \times n$, where K_a is the association constant, M is the macromolecule concentration (i.e., *Tm*GH1 or almond β-glucosidase) and n is the number of binding sites on the macromolecule] were always 1 or greater, allowing accurate deconvolution of the binding parameters. All ITC data were corrected for the heat of dilution of the titrant by subtracting the excess heats at high molar ratios of inhibitor to enzyme. Binding stoichiometry, enthalpy, and equilibrium association constants were determined by fitting the corrected data to a bimolecular interaction model. ΔG_a and ΔS_a were determined using the fundamental equation $\Delta G = -RT \ln K_a = \Delta H - T\Delta S$. Changes in heat capacity (ΔC_p) were determined by the temperature dependence of ΔH_a as described previously.[52] The number of protons released or absorbed (n_{H+}) upon binding of *Tm*GH1 and inhibitor were determined by measuring apparent enthalpies of association (ΔH_a^{app}) in two different buffers (100 mM MES or citrate, pH 5.8) that exhibit significantly different enthalpies of ionization (ΔH_i) according to eq 4.[27] Values of $\Delta H_i = -0.8$ kcal mol^{-1} for citrate and $\Delta H_i = +3.7$ kcal mol^{-1} for MES were used in these calculations.[53]

$$n_{H+} = \frac{\Delta H_a^{app}(\text{buff}_1) - \Delta H_a^{app}(\text{buff}_2)}{\Delta H_i(\text{buff}_1) - \Delta H_i(\text{buff}_2)} \quad (4)$$

Crystallization and X-ray Analysis of *Tm*GH1 and Inhibitor Complexes. Crystals of *Tm*GH1-His$_6$ were grown overnight at 18 °C by the hanging drop method. A 2:1 ratio of enzyme solution (10 mg mL^{-1} in 50 mM imidazole, pH 7) to crystallization buffer (15% PEG 4 K, 0.2 M $CaAc_2$, 0.1 M imidazole, pH 7) proved to be optimal. The crystals were soaked briefly (3−10 s) in crystallization buffer containing 20% glycerol prior to flash freezing in liquid nitrogen. *Tm*GH1-His$_6$ in complex with 2,4-dinitrophenyl 2-deoxy-2-fluoro-β-glucoside, **1**, and **2** were obtained by equilibrating selected crystals in solution containing 10 mM inhibitor (3 mM for 2,4-dinitrophenyl 2-deoxy-2-fluoro-β-glucoside) for 3−5 h. Prior to freezing, the crystals were soaked briefly (3−10 s) in crystallization buffer containing 20% glycerol as above.

X-ray diffraction data, to 2.1 Å resolution, were collected at the European Synchrotron Radiation Source beam-lines ID14-EH4 and ID14-EH2 using an ADSC Quantum-4 CCD as detector. Data were processed and reduced using DENZO/SCALEPACK from the HKL suite.[54] All further computing used the CCP4 suite[55] of programs unless otherwise stated. Despite the equivalence in length of the crystallographic a and b axes, crystals of *Tm*GH1-His$_6$ are in orthorhombic space-group $P2_12_12_1$ with approximate cell dimensions $a = 94.3$ Å, $b = 94.4$ Å, $c = 113.1$ Å, $\alpha = \beta = \gamma = 90°$.

The *Tm*GH1-His$_6$ structure was solved by molecular replacement using the program AMoRe[56] with the *Bacillus circulans* family 1 β-glucosidase, 1qox, as the search model with data from 30 to 4 Å and with an outer radius of Patterson integration of 25 Å. The asymmetric unit contains two molecules of *Tm*GH1-His$_6$, consistent with its dimeric state in solution. Following structure solution, 5% of the observations were set aside for cross-validation analysis[57] and were used to guide refinement strategies such as geometric weighting and the modeling of solvent water. The structures were refined by maximum-likelihood methods using REFMAC[58] with manual correction of the model using QUANTA (Accelrys, San Diego Ca). Refinement of *Tm*GH1-His$_6$ in complex with ligands followed standard procedures, with identical cross-validation reflections maintained, and with ligand geometry target values calculated using QUANTA. Coordinates and observed structure factor amplitudes have been deposited with the

(52) Boraston, A. B.; Creagh, A. L.; Alam, M. M.; Kormos, J. M.; Tomme, P.; Haynes, C. A.; Warren, R. A.; Kilburn, D. G. *Biochemistry* **2001**, *40*, 6240−6247.
(53) Goldberg, R. N.; Kishore, N.; Lennen, R. M. *J. Phys. Chem. Ref. Data* **2002**, *31*, 231−369.
(54) Otwinowski, Z.; Minor, W. *Methods Enzymol.* **1997**, *276*, 307−326.
(55) Collaborative Computational Project Number 4. *Acta Crystallogr.* **1994**, *D50*, 760−763.
(56) Navaza, J.; Saludijan, P. *Methods Enzymol.* **1997**, *276*, 581−594.
(57) Brünger, A. T. *Nature* **1992**, *355*, 472−475.
(58) Murshudov, G. N.; Vagin, A. A.; Dodson, E. J. *Acta Crystallogr.* **1997**, *D53*, 240−255.
(59) Esnouf, R. M. *J. Mol. Graphics* **1997**, *15*, 133−138.
(60) Read, R. J. *Acta Crystallogr.* **1986**, *A42*, 140−149.

Macromolecular Structure Database via the European Bioinformatics Institute (http://www.ebi.ac.uk/msd/). Details of X-ray data and structure quality are given in Table 3.

Acknowledgment. T.G. thanks the EPSRC for provision of a postgraduate fellowship. A.B.B. thanks the Natural Sciences and Engineering Research Council of Canada for a postdoctoral fellowship. The York laboratory is funded by the Wellcome Trust and the BBSRC. R.V.S. thanks the Australian Research Council for financial assistance. G.J.D. is a Royal Society University Research Fellow.

JA036833H